THWAITES' METHOD IN LAMINAR BOUNDARY LAYER

Assoc. Prof. Amer Nordin
Lim Chee Wah
Faculty of Mechanical Engineering
Universiti Teknologi Malaysia

Synopsis

Thwaites' method can be applied to find the boundary layer characteristics for either similar or nonsimilar flow for a variety of boundaries ranging from a simple flat plate (Blasius's Solution[1]) to a symmetrical airfoil. The flow properties to be determined include potential flow velocity distribution, displacement thickness, momentum thickness and coefficient of friction. Furthermore, the location of flow separation is readily obtainable from the numeric value of local coefficient of friction.

Thwaites' Method is able to provide satisfactory approximate solution to different types of simple boundary as long as the flow is laminar and not separated. For a complex curvature such a an airfoil Thwaite' Method is yet to be tested. In this context, we will look into the applicability of Thwaites' Method for a particular symmetrical airfoil, NACA 0012.

Nomenclature

Symbols	Definitions
C	a constant
C_f	coefficient of friction
F	a subsidiary parameter for velocity distribution
H	shape factor
L	characteristic length of body
P	fluid pressure
RL	Reynold's Number
Re	Reynold's Number
U_e	flow velocity outside the boundary layer
U*	dimensionless flow velocity outside the boundary layer
U_∞	velocity of free stream
V	velocity of free stream
l	flow parameter defined by Eq. (A1.14)
m	wedge angle parameter
r	radius of circular cylinder
u	x-component velocity
u*	dimensionless x-component velocity
v	local velocity on the surface of the wing section
x	horizontal or boundary coordinate system
y	vertical or normal coordinate system
α_o	angle of attack
β	wedge angle parameter ($\pi\beta$ = wedge angle)
δ^*	displacement thickness
ε	distance of the centre of circle to the centre of coordinates
ε_T	angular shift of stagnation point of a circle due to circulation
θ	angular coordinate, positive counterclockwise
θ	momentum thickness
λ	flow parameter defined by Eq. (A1.13) or Eq. (A1.15)
τ_w	boundary shear stress

υ	kinematic viscosity
ϕ	angle measured from the stagnation point
ψ	magnitud of the imaginary part of the complex variable w
ψ_o	average value of ψ defined by Eq. (A2.21)

Introduction

Towards the end of the 19th century, the science of fluid mechanics began to diverge into two distinct branches which had practically no points in common. There were the science of theoretical hydrodynamics and the highly empirical science of hydraulics.

Theoretical hydrodynamics fundamentally describes the theory of a hypothetical frictionless and non-viscous fluid, resulting in Euler's equation of motion. Hydraulics, on the other hand, was based on a large number of experimental data. It differed greatly in its methods from the science of theoretical hydrodynamics.

Therefore, scientists in the beginning of the 20th century began to look for a precise and compact solution. In this aspect, L. Prandtl set the milestone by showing the way to unify these two divergent branches of fluid mechanics. He developed a remarkable boundary layer equation deduced from the more general Navier-Stoke's equation of motion. Prandtl discarded complexity by considering the "order" or "weight"[5], of each term in the fluid motion equations. This equation was later pushed a step forward by Von Karman who merged the Prandtl's Boundary Layer Eqaution and the fluid continuity equation to form Vom Karman's Momentum Integral Equation. This equation is simpler because it does not involve partial differential terms.

In solving boundary layer problems, scientists in the early of the 20th century introduced the concept of similarity to certain class of flows and it had been proved very fruitful. "Similar" solution expresses the assumption that two velocity profiles u(x,y) located at different coordinates x differ only by a scale factor in u and y where u is the x-component of the velocity along the boundary.

Historically, the flow along a thin flat plate was the first example illustrating the application of Prandtl's boundary layer theory. By making full use of the concept of flow similarity. Blasius (1907) distinguished himself by solving the flat plate boundary layer problem, ended up with the famous Blasius's Equation in his doctorate's thesis at Goettingen.

A combined method of analysis and experiments is termed semi-emperical, such as Thwaites' Method. Thwaites introduced two flow parameters, l and λ, where

$$\frac{\partial u}{\partial y} = \frac{U_e}{\theta} l$$

$$\lambda = \frac{\theta^2}{\nu} \frac{dU_e}{dx}$$

which relies primarily on experiment data as well as analytical exact solutions.

For about twenty years after its inception by L Prandtl in 1904 (in a paper on "Fluid Flow With Very Small Friction" pesented before the Mathematical Congress in Heidelberg), the boundary layer theory was being developed almost exclusively in his own institute in Goettingen. This period ended with Prandtl's Wilbur Wright Memorial Lecture in 1927 at a meeting of the Royal Aeronautical Society in London. Today, the study of boundary layer theory has spread all over the world, constituting one of the most important pillars in fluid mechanics.

The Application Of Thwaites' Method

Introduction

In this chapter, applicability of Thwaites' Method is investigated for various types of boundary, ranging from a simple shape to a complex feature.

Section 2.2 gives theoretical background of Thwaites' Method and its applicability to provide approximate solution for laminar boundary layers.

Specific attention is given to cater for determination of potential flow velocity distribution over an arbitrary airfoil.

Thwaites' Equation

Thwaites' Equation, as given in [2], can be expressed as

$$\frac{\theta^2 U_e^6}{\nu} = 0.45 \int_o^x U_e^5 \, dx + \left(\frac{\theta^2 U_e^6}{\nu} \right) \qquad \ldots (2.1)$$

In term of dimensionless quantities defined by

$$x^* \equiv \frac{x}{L}, \quad u^* \equiv \frac{u}{U_{ref}}, \quad U_e^* \equiv \frac{U_e}{U_{ref}}, \quad R_L \equiv \frac{U_{ref} L}{\nu}$$

Eq. (2.1) can be rewritten as

$$\left(\frac{\theta}{L} \right)^2 R_L = \frac{0.45}{\left(U_e^* \right)^6} \int_o^x \left(U_e^* \right)^5 dx^* + \left(\frac{\theta}{L} \right)^2_{x=0} R_L \left(\frac{\left(U_e^* \right)_{x=0}}{U_e^*} \right)^6 \qquad \ldots (2.2)$$

By collecting known solutions of Prandtl's Boundary Layer Equation, Thwaites plotted H and *l* as functions of λ as shown in Figure 1 below, where H is the shape factor and *l* and λ are two flow parameters.

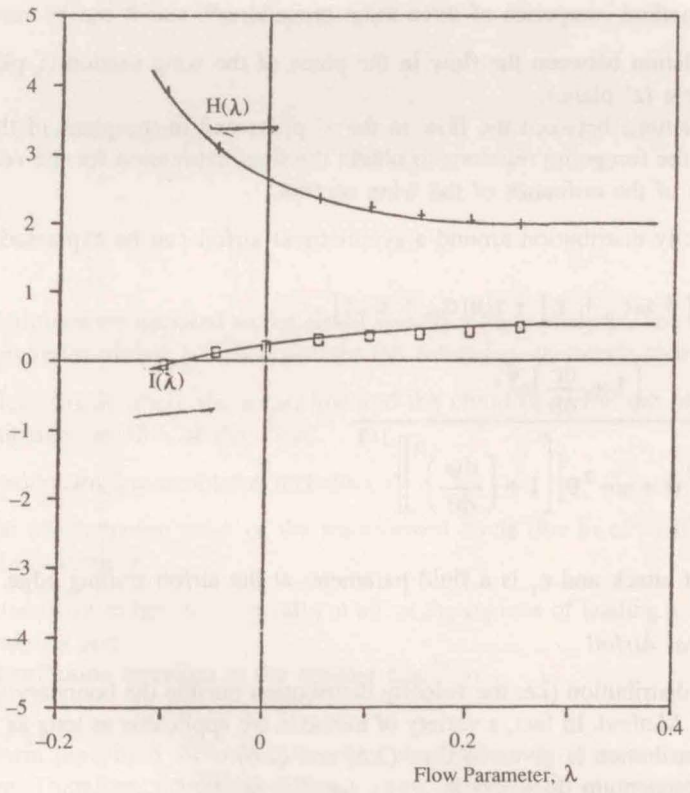

Figure 1 Functions in Thwaites' Method

The two functions in Graph 1 may be fitted by the following equations,

$-0.1 \le \lambda \le 0$	$0 \le \lambda \le 0.1$
$l = 0.22 + 1.420\lambda + \dfrac{0.018\lambda}{0.107 + \lambda}$ ... (2.3a)	$l = 0.22 + 1.57\lambda - 1.8\lambda^2$ ... (2.3b)
$H = \dfrac{0.0731}{0.14 + \lambda} + 2.088$ ... (2.4a)	$H = 2.61 - 3.75\lambda + 5.24\lambda^2$ ... (2.4b)

Validity of Thwaites' Method for Simple Boundaries

The application of Thwaites' Method has been found satisfactory for various types of simple boundaries such as a flat plate, a wedge or a circular cylinder. Tables of result and certain significant graphs of this approximate method are included in the appendix.

Velocity Distribution Over An Arbitrary Airfoil

In order to apply most existing methods to determine boundary layer properties, the potential flow velocity must first be known. Equivalently, the boundary effect is not accounted for initially, i.e. the boundary is assumed frictionless.

The potential velocity distribution of an arbitrary can be derived from the potential flow theory. A double-transformation is introduced which includes;

1) Joukowski Transformation,
2) An infinite Fourier Series Transformation due to Theodorsen.

The skeleton of the method comprises of three main procedures[6] and it can be summarized as;

i) Derivation of relation between the flow in the plane of the wing section (ζ-plane) and in the plane of the distorted circle (z' plane),
ii) Derivation of relations between the flow in the z' plane and in the plane of the true circle (z plane),
iii) Combination of the foregoing relations to obtain the final expression for the velocity distribution in the ζ plane in terms of the ordinates of the wing section.

The potential flow velocity distribution around a symmetrical airfoil can be expressed as

$$\frac{v}{V} = F\left[\sin[\theta + \alpha_o + \varepsilon] + \sin[\alpha_o + \varepsilon_T]\right] \quad \ldots (2.5)$$

where

$$F = \frac{\left(1 + \dfrac{d\varepsilon}{d\theta}\right)e^{\psi_o}}{\left\{\left[\sinh^2\psi + \sin^2\theta\right]\left[1 + \left(\dfrac{d\psi}{d\theta}\right)^2\right]\right\}^{1/2}} \quad \ldots (2.6)$$

where α_o is the angle of attack and ε_T is a fluid parameter at the airfoil trailing edge.

Flow Over A Symmetrical Airfoil

The external-velocity distribution (i.e. the velocity distribution outside the boundary layer) is a prerequisite in order to apply Thwaites' Method. In fact, a variety of methods are applicable as long as this specific prerequisite is met. This velocity distribution is given in Eqs. (2.5) and (2.6).

From Eq. (2.2), the momentum thickness is

$$\frac{\theta}{L}\sqrt{R_L} = \left[\frac{0.45}{(U_e^*)^6}\int_o^x (U_e^*)^5\, dx^*\right]^{1/2} \quad \ldots (2.7)$$

Numerical integration may be performed by using the trapezium rule, which is a numerical integration method to find the area bounded by a curve and the axes. Eq. (2.7) becomes

$$\frac{\theta}{L}\sqrt{R_L} = \left[\frac{0.45}{(U_e^*)^6}\sum_{r=1}^{2\pi}\frac{(U_{e_r}^* + U_{e_{r-1}}^*)\Delta x^*}{2}\right]^{1/2} \quad \ldots (2.8)$$

An approximation of shape function H is given in Eq. (2.4). Shape function relates displacement thickness and momentum thickness. Therefore, known values of H and momentum thickness ensure a complete knowledge of displacement thickness. The displacement thickness may be expressed as

$$\left(\frac{\delta^*}{L}\right)\sqrt{R_L} = H\frac{\theta}{L}\sqrt{R_L} \quad \ldots (2.9)$$

This equation provides direct computation of non-dimensional displacement thickness.

To compute the coefficients of friction along an airfoil boundary, we apply the same concept as descriped previously. Nevertheless, a function of flow parameter, $l(\lambda)$ as given in Eq. (2.3), is included instead of H. The coefficient of friction is

$$\frac{C_f L}{\upsilon R_L} = \frac{2l(\lambda)}{U_e^*\left(\frac{\theta}{L}R_L\right)} \quad \ldots (2.10)$$

The location of flow separation may be deduced from a series of coefficient of friction as given in Eq. (2.10). It is defined as a point on a solid boundary with null friction.

$$C_f = 0$$

or

$$\frac{C_f L}{\upsilon R_L} = 0 \quad \ldots (2.11)$$

determines the point of flow separation.

Analysis

Conditions Of Analysis

Some fundamental conditions are imposed on the airfoil boundary layer analysis. The specific airfoil considered is NACA 0012, a 4-digit series airfoil, which possesses the following geometric characteristics;

i) It is a symmetrical airfoil where the mean line and the chord of airfoil are identical,
ii) Its maximum thickness is 12% of the chord.

Besides, the basic aerodynamic assumptions include,

i) The angular shift of stagnation point of the transformed circle due to circulation, ε_T, is zero,
ii) The flow is entirely laminar.

The analysis is not reliable, or rather to say invalid at all, at the regions of leading and trailing edges. The two main causes of this invalidity are;

i) The thickness distribution equation at the leading edge[3] is
$r_t = 1.1019\ t^2$
ii) In order to perform numerical differentiation there are not enough data at the vicinity of leading edge and trailing edge. Therefore, numerical differentiation at both ends of the airfoil is not accurate.

A series of flow data is obtained for various angles of attack ranging from –0.20 rad to 0.12 rad (–11.46° to 6.88°). All aerodynamics parameters are made dimensionless in order to gain generality.

General Discussion

From a series of numerics for flow over NACA 0012 at various angles of attack (ranging from –0.20 rad to 0.12 rad), we may summarized the following facts;

i) The momentum thickness and the displacement thickness increase along the airfoil boundary and as the angle of attack increases,

ii) The coefficient of friction increases as the angle of attack increases but it decreases along the airfoil boundary,

iii) The location of flow separation at the upper boundary keeps moving forward as the angle of attack increases. For the lower surface, location of flow separation is unreliable whereby the causes of unreliability might be;

a) λ is out of range of reliable data,

b) numerical error while performing numerical differentiation or integration, or during the process of transformation from an airfoil to a circle.

Table 1 shows a series of location of separation point for various angles of attack ranging from –0.10 rad to 0.15 rad (–5.73° to 8.59°).

Table 4.1 Locations of Separation point

angle of attack α (rad)	location of separation point x_{le} (% of chord)	
– 0.10	0.7803	to be reviewed
– 0.09	0.7846	
– 0.08	0.7904	
– 0.07	0.7929	
– 0.06	0.7905	
– 0.04	0.7800	
– 0.03	0.7321	
– 0.02	0.7140	
– 0.01	0.6705	
0.00	0.6380	
0.01	0.5886	
0.02	0.5393	
0.03	0.4827	
0.04	0.4391	
0.05	0.3748	
0.06	0.3069	
0.07	0.2347	

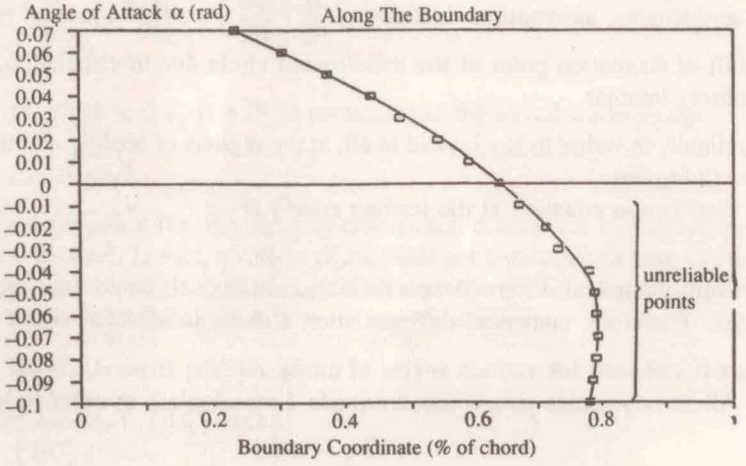

Figure 2 Location of separation

Effects Of Flow Separation

Flow separation occurs for positive pressure gradient, $\frac{\partial P}{\partial x} > 0$, along the boundary of a body. Therefore, only flat and convex surfaces can develop flow separation. A concave surface has negative pressure gradient. Therefore, flow will never separate for this type of curvature.[4]

When a body with convex boundary is immersed in a flowing fluid, the static pressure increases rapidly in the streamline direction. A dramatic and undesirable change in the flow pattern happens. Streamlines in the boundary layer near the surface suddenly departs from the surface. This flow separation is undesirable because the body was designed to produce a given static pressure variation for a specific purpose, such as to produce lift for an airfoil or to provide efficient deceleration of a flow in a diffuser. If the flow separates, the intended static pressure distribution will obviously be disrupted. Furthermore, flow separation will disturb an intended distribution of heat or mass transfer.

When a flow separates, the viscous region is no longer thin, even at high Reynolds numbers, and the boundary layer assumptions are no longer valid. Thus, the conditions for the applicability of the boundary layer assumption must be high-Reynolds-number flow over streamlined boundaries.

Conclusion

Thwaites' Method provides a much simpler way to find the boundary layer properties for fluid flow over a variety of two dimensional obstacles as long as velocity outside the boundary layer $U_e(X)$ is known[2]. It discards complicated numerical calculation and reveals approximate solutions.

However, applicability of Thwaites' Method is very much dependent on the validity of λ, a flow parameter. Extension of the relationship between λ, flow parameter $l(\lambda)$ and shape function $H(\lambda)$ helps to generalize this method.

References

1. Schlichting, H., *Boundary-layer Theory*, McGraw-Hill Book Company, U.S.A., pg. 135 & 141, 1979.
2. Cebeci, T. & Bradshaw, P., *Momentum Transfer In Boundary Layer*, Hemisphere Publishing Corporation, U.S.A., pg. 108-112, 1977.
3. Abbott, I.H. & Doenhoff, A.E., *Theory of Wing Section*, Dover Publications, Inc., pg. 113-115, 1959.
4. Schlichting, H., *Boundary-layer Theory*, McGraw-Hill Book Company, U.S.A., pg. 131-133, 1979.
5. Cebeci, T. & Bradshaw, P., *Momentum Transfer In Boundary Layer*, Hemisphere Publishing Corporation, U.S.A., pg. 39-44, 1977.
6. Abbott, I.H. & Doenhoff, A.E., *Theory of Wing Section*, Dover Publications, Inc., pg. 53-60, 1959.

Appendix 1 Boundary layer flow parameters of wedge-flow

Flow Parameter λ	Pressure Gradient m	Wedge Angle β (rad)	L(lamda) $L(\lambda)$	H(lamda) $H(\lambda)$	Momentum Thickness $\frac{\theta}{x}\sqrt{Re_x}$	Displacement $\frac{\delta^*}{x}\sqrt{Re_x}$	Friction Coefficient $C_f\left(\frac{U_\infty}{U_e}\right)^2$
-0.1000	-0.1053	-0.7392	-0.0601	3.9111	0.9747	3.8120	-0.1232
-0.0910	-0.1006	-0.7024	-0.0025	3.6601	0.9513	3.4819	-0.0053
-0.0905	-0.1003	-0.7003	0.0001	3.6485	0.9500	3.4661	0.0003
-0.0900	-0.1000	-0.6981	0.0027	3.6371	0.9487	3.4504	0.0058
-0.0500	-0.0714	-0.4833	0.1203	3.0888	0.8367	2.5843	0.2875
0.0000	0.0000	0.0000	0.2095	2.6430	0.6708	1.7729	0.6246
0.0500	0.2500	1.2566	0.3006	2.3558	0.4472	1.0535	1.3442
0.0750	1.0000	3.1416	0.3350	2.2908	0.2739	0.6274	2,4466
0.0900	*******	6.2832	0.3508	2.2630	.0000	.0000	*******
0.1000	-2.0000	12.5664	0.3596	2.2448	ERR	ERR	ERR
0.1500	-0.5000	-6.2832	0.3902	2.1218	ERR	ERR	ERR
0.2000	-0.3636	-3.5904	0.4199	2.0735	ERR	ERR	ERR
0.2500	-0.3125	-2.8560	0.4800	2.0312	ERR	ERR	ERR

*** – ∞

ERR – complex number

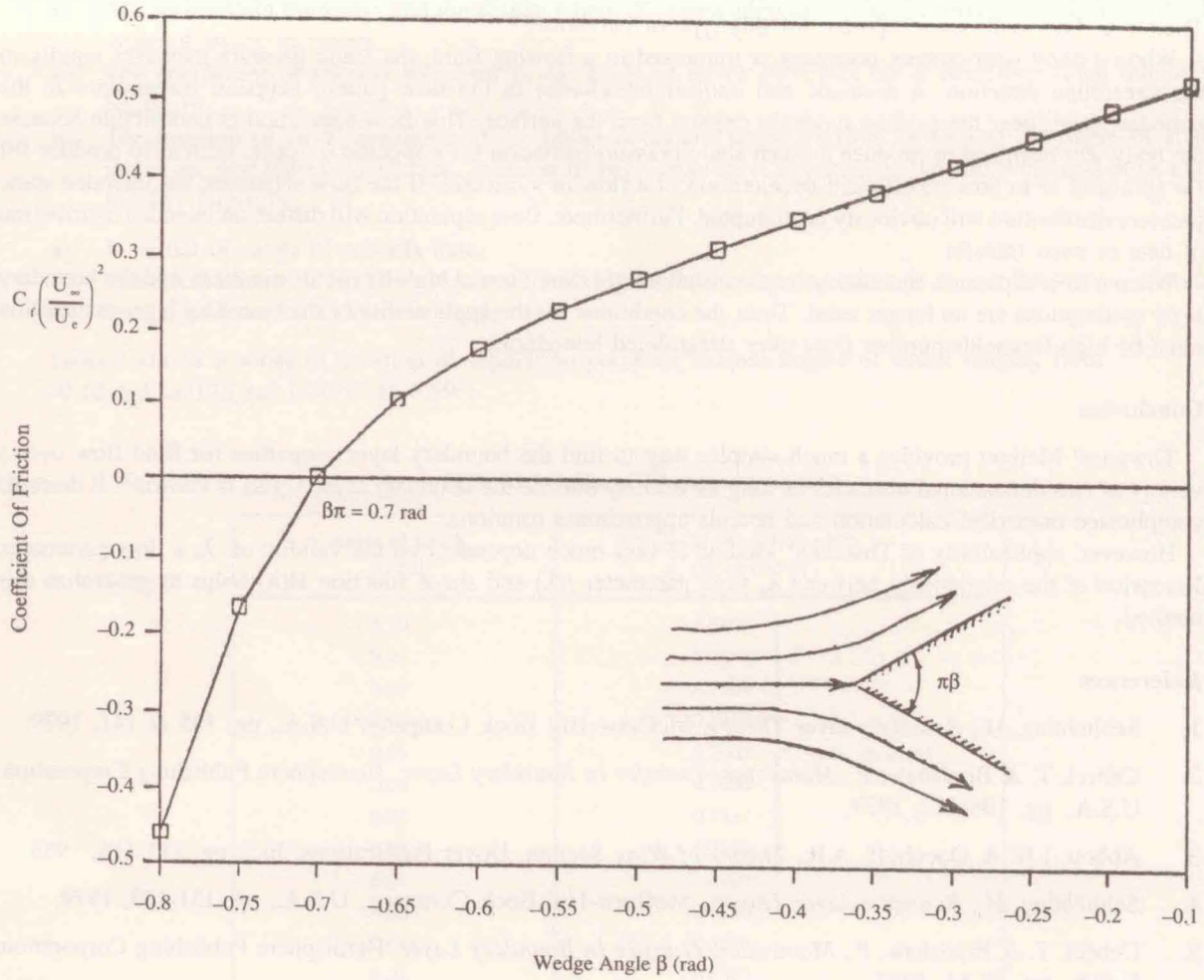

Figure 3 Flow over a wedge

Appendix 2 Boundary layer flow parameters of flow over a circular cylinder

phi (deg)	phi (rad)	lamda	L (lamda)	H (lamda)	momentum thickness	displsacement thickness	friction coefficient Cf
0.00	0.000000	ERR	ERR	ERR	ERR	ERR	ERR
10.00	0.174533	0.074711	9,334672	2.291381	0.194761	0.446272	1.193607
20.00	0.349066	0.073805	0.333598	2.293208	0.198168	0.454442	2.303106
30.00	0.523599	0.072150	0.331602	2.296616	9,204098	0.468734	3.249540
40.00	0.698132	0.069488	0.328296	2.302311	0.212968	0.490318	3.963625
50.00	0.872665	0.065350	0.322924	2.311779	0.225463	0.521221	4.388873
60.00	1.047198	0.058889	0.313973	2.328392	0.242670	0.565032	4.482076
70.00	1.221730	0.048519	0.298215	2.360960	0.266326	0.628785	4.208966
80.00	1.396263	0.031107	0.268399	2.436423	0.299279	0.729171	3.532884
90.00	1.570796	.000000	0.209510	2.642950	0.346410	0.915545	2.419288
100.00	1.745329	– 0.060263	0.100386	3.191840	0.416558	1.329588	0.949345
103.00	1.797689	– 0.088815	0.008770	3.610792	0.444309	1.604306	0.076929
103.10	1.799434	– 0.089887	0.003332	3.634513	0.445302	1.618454	0.029156
103.15	1.800307	– 0.090426	0.000516	3.646792	0.445800	1.625739	0.004509
103.20	1.801180	– 0.090967	– 0.002368	3.659361	0.446299	1.633170	– 0.508234
104.00	1.815142	– 0.099927	– 0.059508	3.908655	0.454452	1.776296	– 0.508234
105.00	1.832596	– 0.111970	– 0.172870	4.412022	0.465090	2.051988	– 1.436153
110.00	1.919862	– 0.189921	– 3.978187	24.753765	0.526921	13.043802	– 28.379126

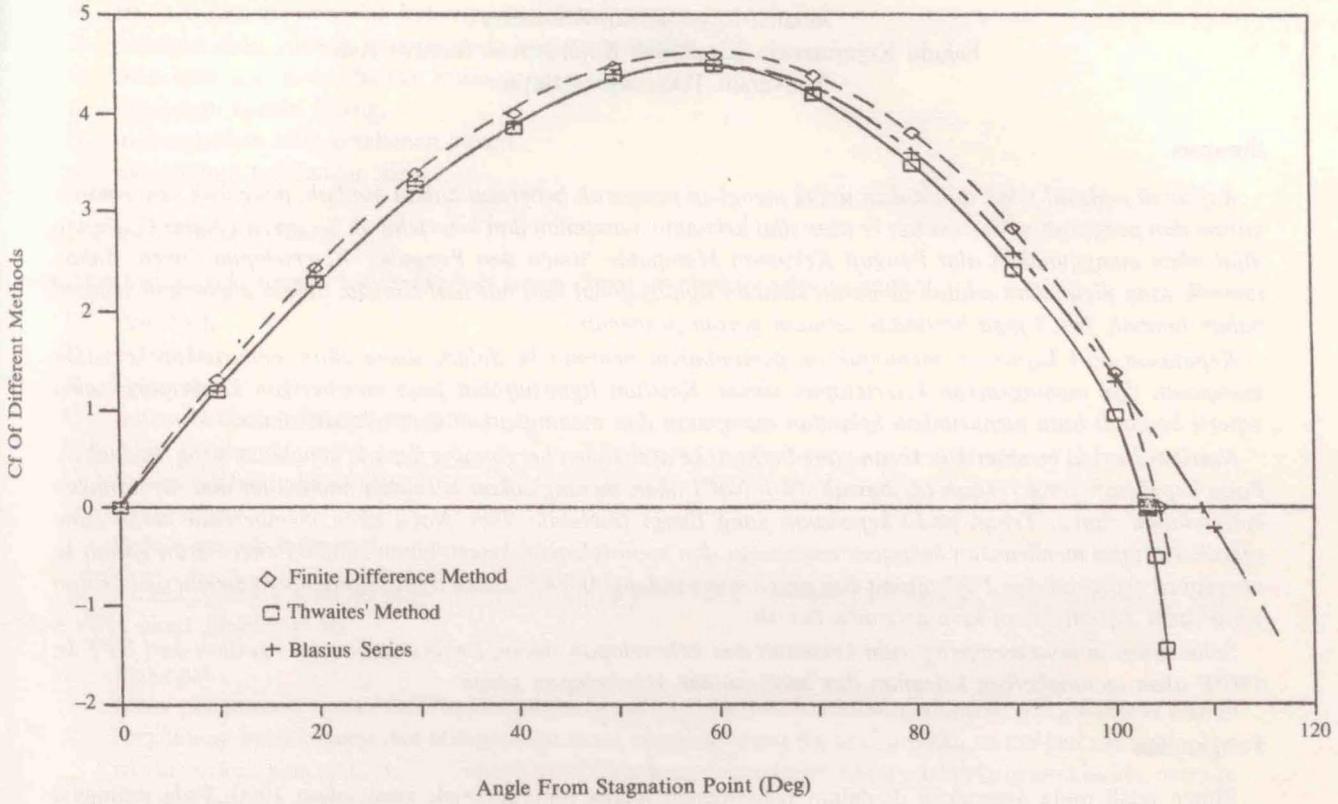

Figure 4 Cf for flow over a circular cylinder

Appendix 3 Comparison

	Exact Solution	Approximate Solution (Thwaites' Method)
Flate Plae	$\frac{\delta^*}{x} = \frac{1.721}{\sqrt{Re_x}}$ $C_f = \frac{0.664}{\sqrt{Re_x}}$	$\frac{\delta^*}{x} = \frac{1.771}{\sqrt{Re_x}}$ $C_f = \frac{0.626}{\sqrt{Re_x}}$
Wedgw Flow	Separation wedge angle $\beta\pi = -0.629$ rad	Separation wedge angle $\beta\pi = -0.698$ rad
	Dimensionless pressure gradient parameter $m = -0.091$	Dimensionless pressure gradien parameter $m = -0.100$
Circular Cylinder	Separation angle $\phi = 108.8°$	Separation angle $\phi = 103.2°$